J Nanostruct 16(4): 4643-4650, Autumn 2026

RESEARCH PAPER

Structural, Morphological, and Optical Properties of Si Quantum Dot-Doped Cs_2NaBiI_6 Lead-Free Double Perovskites

Muna Saeed Owayez [1] *, *Majid R. Al-bahrani* [2], *Haidar Gazy Al-sabah* [1]

[1] *Department of General Science, College of Basic Education, Misan University, Iraq*

[2] *Laboratory of Nanomaterials and Plasma, College of Science, University of Thi-Qar, Thi Qar, Iraq*

ARTICLE INFO

Article History:
Received 23 April 2026
Accepted 12 July 2026
Published 01 October 2026

Keywords:
Cs_2NaBiI_6 perovskite
Lead-free
Nanocomposite
SiQDs

ABSTRACT

The intensifying need for the removal of hazardous lead from perovskite optoelectronics has spurred thorough investigation into environmentally benign replacements, but lead-free perovskites are historically limited by low stability under ambient conditions and less than ideal optoelectric performance Herein, we disclose a pioneering approach to remedy these problems via compositional engineering of silicon quantum dots (SiQDs) as well as their controlled incorporation onto the surface of the lead-free double perovskite matrix Cs_2NaBiI_6. Using a simple hydrothermal synthesis route, we systematically studied the influence of the doping of SiQDs at low (1%,3%, and 5%) concentrations on the structural, morphological and optical characteristics of the host material. Through X-ray diffraction (XRD), field-emission scanning electron microscopy (FESEM), transmission electron microscopy (TEM), ultraviolet-visible (UV-Vis) spectroscopy, and Fourier-transform infrared (FTIR) spectroscopy comprehensive characterizations demonstrate that the optimal doping of SiQDs is 3%. With this high concentration of SiQDs, pronounced grain refinement (down to 100 nm), improved crystallinity, efficient defect passivation and a blue bathochromic shift in the absorption edge work together for the better light-harvesting characteristics. In contrast, 5% over doping results in quantum dot agglomeration and interfacial degradation that severely decrease the optoelectronic performance. Our findings described herein establish SiQDs-mediated engineering as a robust, sustainable means to industrially harness the interplay between individual components of lead-free perovskite systems to maximize performance; thereby unlocking promising candidates—like Cs_2NaBiI_6 for next-generation, scale-invariant and green photovoltaics and optoelectronic devices.

How to cite this article
Saeed Owayez M, R. Al-bahrani M, Gazy Al-sabah H . Structural, Morphological, and Optical Properties of Si Quantum Dot-Doped Cs_2NaBiI_6 Lead-Free Double Perovskites. J Nanostruct, 2026; 16(4):4643-4650. DOI: 10.22052/JNS.2026.04.014

INTRODUCTION

Lead halide perovskites have been well-known to exhibit excellent photoelectric properties and device performance in optoelectronics [1]. However, their intrinsic instability and toxicity issues prevent them from being commercially viable. This has led to an extensive search for Pb-free materials with similar favourable optoelectronic properties. Lead-free double perovskites (DPs) have emerged as one of the most

* *Corresponding Author Email: muna75926@gmail.com*

promising candidates that not only fulfill enhanced stability; but also exhibit significantly less toxicity [2]. Their general chemical formula is that of the double perovskites (DPs) howe- ver lead-free, $A_2B^+B^{3+}X_6$ where (Pb^{2+}) cations are replaced with a pair either B^+ and B^{3+} metal one being notigry [3]. Layered double perovskites (LDPs) have further expanded this family of materials, typically expressed as $A_4B^+_2B^{3+}_2X_{12}$. Much interest has been devoted to their layered architectures and the increased tunability of electronic properties provides expanded application possibilities for perovskite-influenced materials [4,[5]. Thus, current high-quality nanocrystals (NCs) of lead free DPs have been widely studied and applied in multiple optoelectronic devices such as light-emitting diodes (LEDs) [6], photodetectors for ultraviolet and X-ray radiation, and solar cell architectures [7,8].

The quest for lead-free double perovskite nanocrystals (DP NCs) with high optical properties has led to multiple synthetic strategies that allow careful control over composition, morphology and crystalline perfection. Of these, direct synthetic routes have been most common with hot-injection technique being used often [9,10]. A significant challenge, however, arises from the multi-elemental composition of DPs. Reactions conducted at elevated temperatures can promote the formation of undesirable impurity phases and side products, compromising the phase-purity of the final material [12,13]. This intrinsic limitation of direct, high-temperature synthesis has in turn inspired the search for alternative indirect synthetic routes to better control over reaction pathways and product quality [14,15].

Embedding quantum dots (QDs) into perovskite compounds has many general benefits for optoelectronic applications. Firstly, QDs enhance the surface morphology by bridging the gaps between grain boundaries and helping in forming a uniform film, which leads to delivering the appropriate movement of charge carriers [15,16]. Second, QDs use appropriate bridging ligands to form stable chemical bonds with the perovskite matrix to passivate surface defects and hide non-radiative recombination [17]. Third, QDs can increase the ability to harvest light energy, (that is) increasing the overall absorbance intensity at each wavelength and the absorption spectrum subsequence broadening or red shift of J-V due to carrier generation over a wide range of photon energies. Fourth, the quantum confinement effect in QDs grants them size-tunable bandgap engineering and easily modifiable composite electronic properties. Fifth, the incorporation of QDs enhances charge extraction and transfer kinetics by forming high-quality percolation

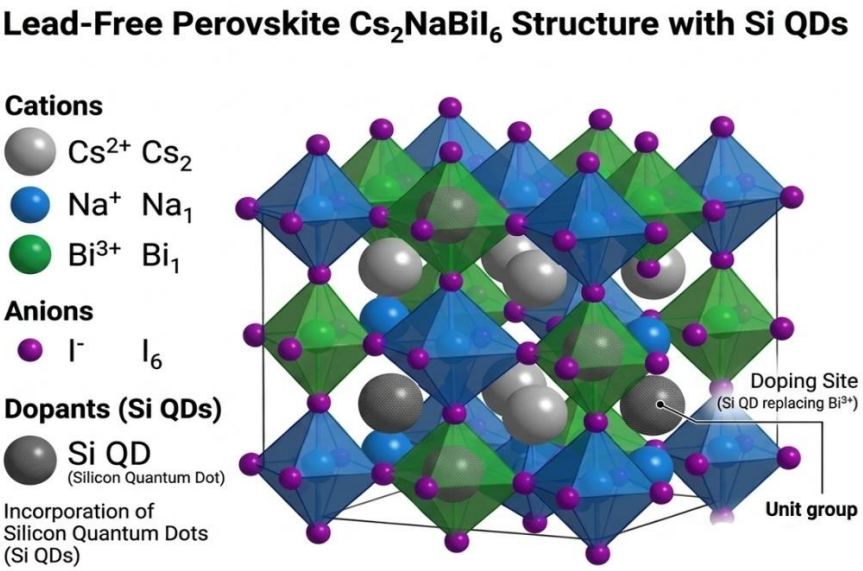

Fig. 1. The crystalline structure of the lead-free double perovskite compound Cs_2NaBiI_6 incorporated with silicon quantum dots (Si QDs).

pathways across the perovskite-QD interface [17,18]. Lastly, the presence of QDs helps in better environmental stability due to their insulating nature protecting against moisture and atmospheric spoilage. Individually, these benefits place quantum dots as a potential additive class to produce high-performing, stable and lead-free perovskite-based optoelectronics [20].

MATERIALS AND METHODS

Cs_2NaBiI_6:Si QDs Nanocomposite Synthesis

The double perovskite compound Cs_2NaBiI_6 is a new lead-free material that was synthesized by solution methods using dimethyl sulfoxide (DMSO) as solvent and stoichiometric amounts of the precursors; 0.87 g of CsI, 0.25 g NaI, and 0.98 g BiI_3 were weighed from high-purity salts (99% purity) before synthesis напрямую? To allow complete dissolution and homogenous reaction, the reaction mixture was stirred at 80 °C for 2 hours followed by cooling to room temperature for precipitation of the pristine perovskite. Then the silicon quantum dots (Si QDs) at three doping concentrations, including 1 wt% (0.0210 g), 3 wt% (0.0630 g) and 5 wt% (0.1050 g), relative to the total perovskite mass, were incorporated into the as-prepared Cs_2NaBiI_6 matrix to obtain composite systems Cs_2NaBiI_6:Si QDs (1%, 3% and 5%). This systematic doping protocol provides a comprehensive avenue to study the impact of incorporation of Si QDs on the structural, optical and electronic properties of Cs2NaBiI6 perovskite for next-generation optoelectronic applications. Fig. 2 shows a schematic description of the stepwise synthesis process followed to obtain both pristine and doped compounds.

RESULTS AND DISCUSSION

SEM and TEM Analysis of Perovskite Nanocomposite

The scanning electron microscopy (SEM) images for the surface morphology of the pristine and doped perovskite samples are presented in Figs. 3a–d. The images in the Fig. 3a show that there is relatively homogeneous, compact,

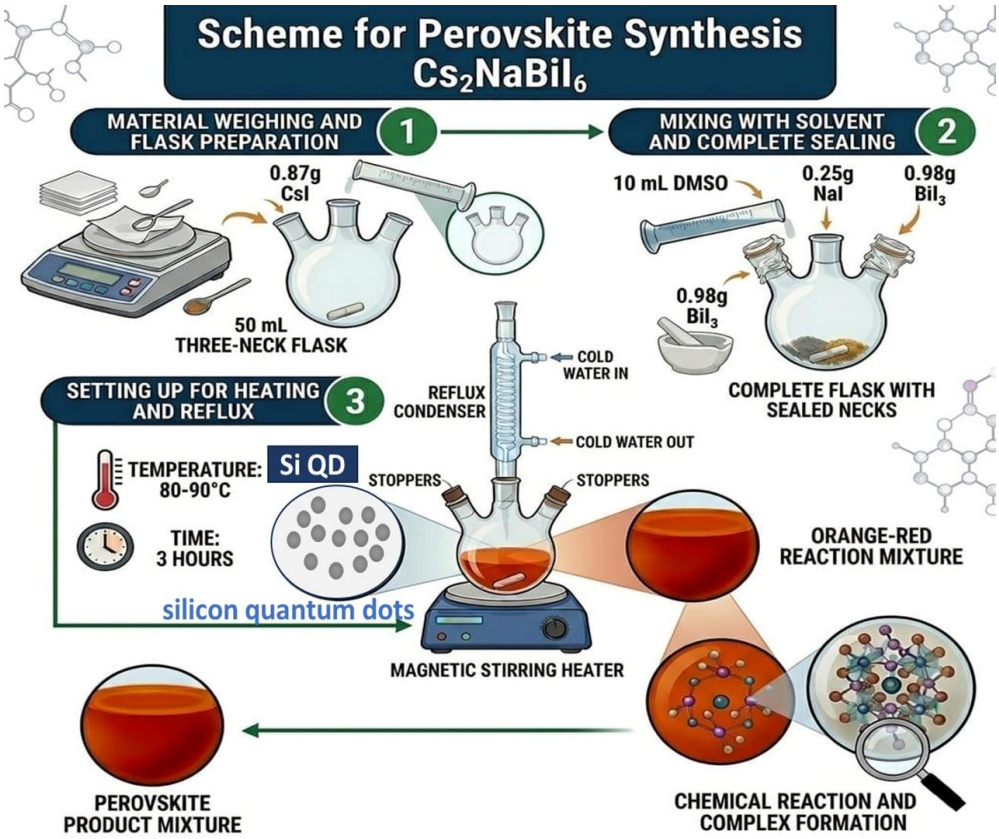

Fig. 2. Scheme for Perovskite Synthesis Cs_2NaBiI_6.

crystalline surface morphology with delineated boundaries between grains and almost no porosity, which indicates that the film can be well- formed as a continuous perovskite layer suitable for optoelectronic devices. In contrast, the surface morphology of (1 wt% Si QDs) in Fig. 3b is similar to that of (0.5 wt% Si QDs), but small clusters from a secondary phase appear on the surface, indicating an initial successful incorporation of Si QDs without major disruption of the perovskite matrix. Fig. 3c, with 3 wt% Si QDs in the nanocomposite systems show the most suitable doping concentration, resulting in uniform dispersion of well-integrated nano composite silica QDs overlaying on Cs_2NaBiI_6 surface; which increases surface coverage while decreasing grain boundary gap and allowing for a relatively favorable rough topography to promote carrier transport and light harvesting. However, Fig. 3d (5 wt% Si QDs) shows severe surface morphology degradation, including obvious aggregation of Si QDs, large irregular clusters with deep cracks and loss of flatness from the corresponding XRD patterns indicating that strong phase separation as well as defect density is increased by over doping. Thus, the best-controlled microstructure is observed in the composite doped with 3 wt% Si QDs for semiconductor device utilization in PSCs and anticipated improvements in power conversion efficiency through improved interfacial contacts, charge extraction or recombination suppression enabled by well-dispersed Si QDs etc., where a lower doping may increase performance while excessive will generally degrade morphology such as at 5 wt% occurrence of shunt paths or carrier trapping impacts negatively on overall

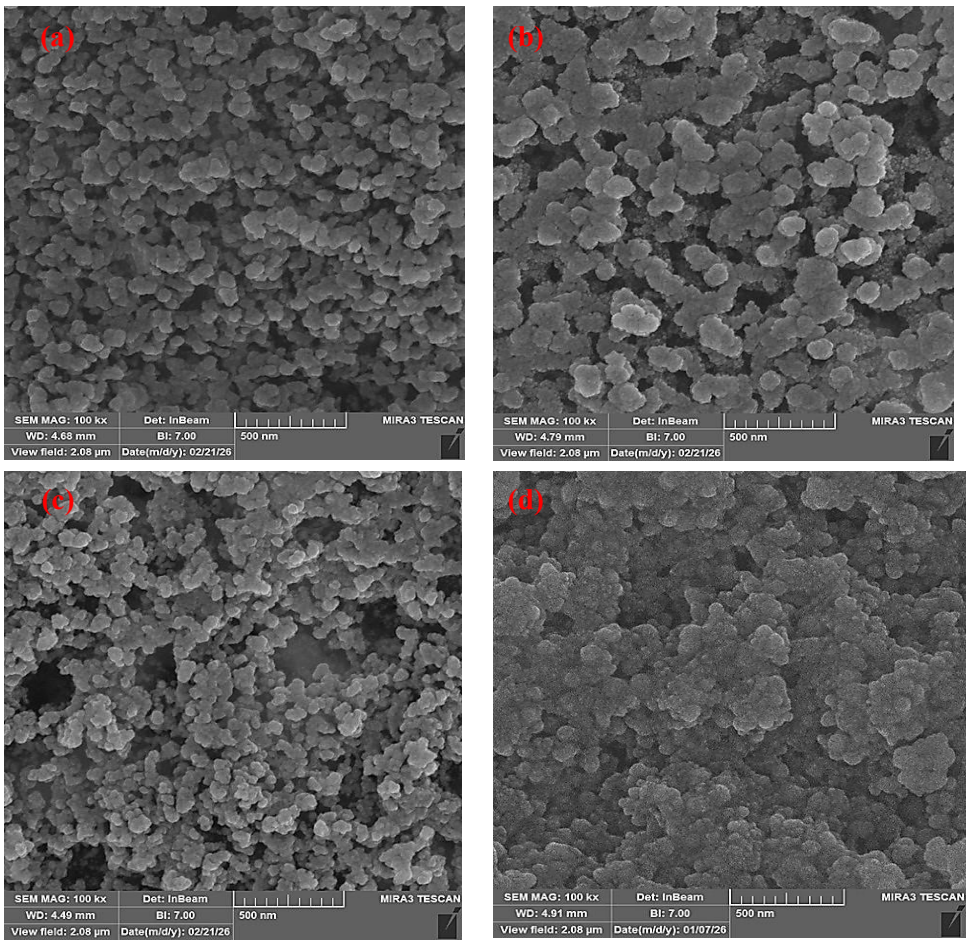

Fig. 3. (a–d) SEM micrographs of pristine Cs_2NaBiI_6 (a), and Cs_2NaBiI_6 doped with 1 wt% (b), 3 wt% (c), and 5 wt% (d) Si QDs.

input/output characteristics.

We examined the characterization of surface morphology and internal nanostructure using the field emission scanning electron microscopy (SEM, Fig. 3) and transmission electron microscopy (TEM, Fig. 4) for the pristine Cs_2NaBiI_6 and crystalline Cs_2NaBiI_6:Si QDs. The SEM images hint the pristine sample (a of Fig. 3) shows a solid, continuous and crystallizes surface with clear grain boundaries while the correspondence TEM image (a) proves that there are no secondary phase or embedded nanoparticle where only pure lattice fringe matching to phase-pure Cs_2NaBiI_6exists as shown in the corresponding (b) of Fig. 4. For the 1 wt% Si QDs doped sample (Fig. 3b, SEM; Fig. 4b, TEM), SEM also indicates formation of small secondary clusters on the surface, and analysis by transmission electron microscopy (TEM) shows isolated Si QDs having diameters of about 3–5 nm dispersed within the perovskite matrix with very little aggregation suggesting that initial successful incorporation has occurred. The highest doping concentration at 3 wt % Si QDs (Fig. 3c, SEM; Fig. 4c, TEM) reveals ~100% surface coverage with limited grain boundary gaps from SEM and homogeneous dispersion across the perovskite bulk as confirmed by TEM with close intimate contact of Si QDs with the Cs_2NaBiI_6 lattice resulted in good charge transfer pathways. For 5 wt% Si QDs (Fig. 3d, SEM; Fig. 4d, TEM), however, the surface of films is found by SEM to suffer from serious deterioration including large irregular agglomerates and cracking, while TEM confirms that excessive aggregation of Si QDs has occurred in those films forming clusters larger than 50 nm together with voids and dislocation

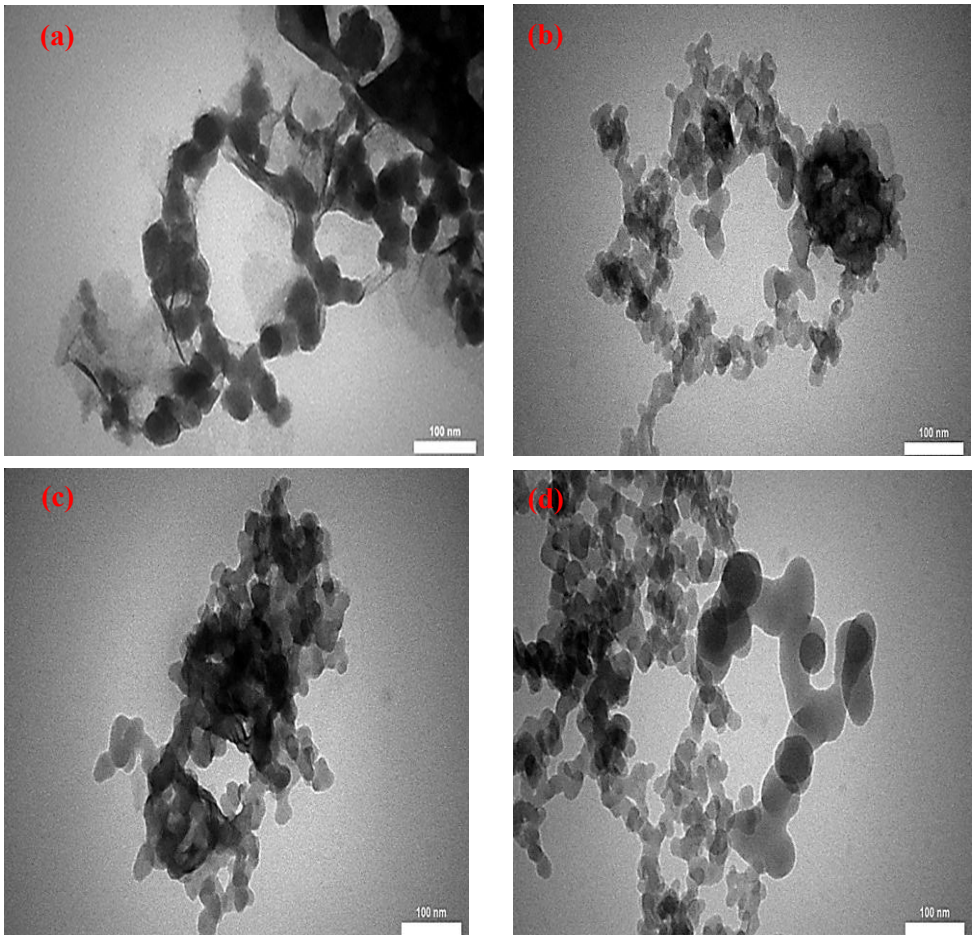

Fig. 4. (a–d) TEM micrographs of pristine Cs_2NaBiI_6 (a), and Cs_2NaBiI_6 doped with 1 wt% (b), 3 wt% (c), and 5 wt% (d) Si QDs.

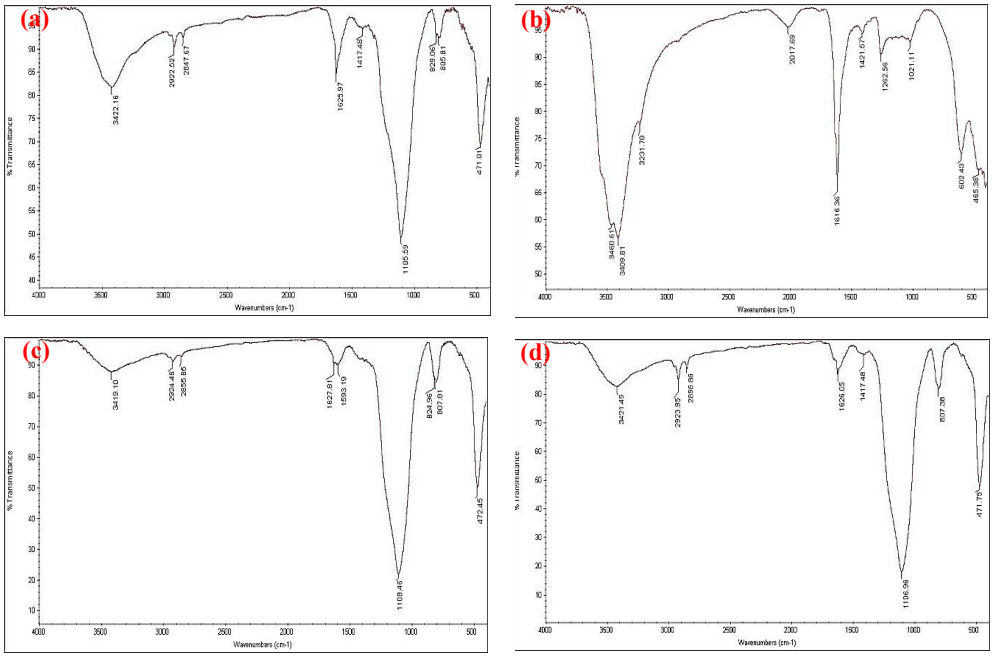

Fig. 5. (a–d) Fourier-transform infrared (FTIR) spectroscopy of pristine Cs_2NaBiI_6 (a), and Cs_2NaBiI_6 doped with 1 wt% (b), 3 wt% (c), and 5 wt% (d) Si QDs.

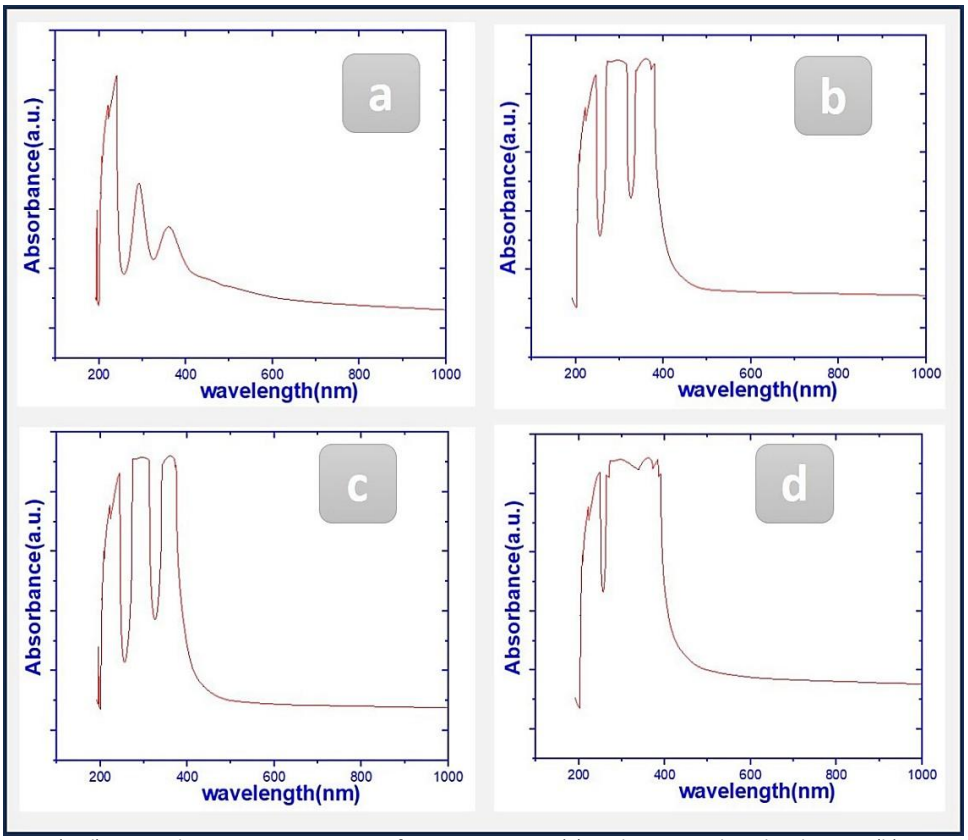

Fig. 6. (a–d) UV-Vis absorption spectroscopy of pristine Cs_2NaBiI_6 (a), and Cs_2NaBiI_6 doped with 1 wt% (b), 3 wt% (c), and 5 wt% (d) Si QDs.

networks indicating phase segregation and loss of structural integrity. Combining both techniques, only the 3 wt% Si QDs sample reaches an optimal compromise between semiconducting properties and surface morphology where the surface states are limited, while providing order at scales smaller than those at which laser light interacts (EQE), without compromising overall crystallinity or introducing defects. Contrary wise, aggregates of Si QDs are detrimental in 5 wt% where the solubility limit of Si QDs in Cs_2NaBiI_6 is exceeded which manifests as surface clusters (SEM) or bulk aggregates (TEM). From the viewpoint of practical photovoltaic devices, especially in PSCs, the 3 wt% Si QDs-doped composite is found to be optimal and possesses benefits such as well dispersed Si QDs which conduce charge transport nanochannels reducing trap-state density light scattering improving stabilized power conversion efficiency (PCE) and device stability Whereas due to agglomerated morphology of the 5 wt% sample results in bad carrier recombination paths shunt pathways leading to rapid degradation of device.

Optical Analysis of Perovskite Nanocomposite

The chemical bonding and the interplay at the interface in pristine Cs_2NaBiI_6 perovskite and their composites containing various weight percentages (1, 3 and 5 wt%) of Si quantum dots were probed by Fourier-transform infrared (FTIR) spectroscopy as illustrated in Fig. 5. As shown in Fig. 5a, the pristine Cs_2NaBiI_6 displays absorption bands below 800 cm^{-1} with a strong band at1847 cm^{-1} due to $[\ BiI_6\ ]^{3-}$ octahedral stretching and bending; this reveals the successful formation of double perovskite. New bands appear at approximately 1021–1105 cm^{-1} assigned to asymmetric stretching vibrations of Si–O–Si and Si–O–Cs/Na linkages in the presence of as little as 1 wt% Si QDs (Fig. 5b), suggesting that, even at this low loading, some initial chemical grafting of Si QDs in silicate mesh forms via oxygen bridges between the network making perovskite matrix. Fig. 5c (3 wt% Si QDs) indicates the most distinct and clear Si–O-related bands while showing broad O–H stretching bands around 3400–3440 cm^{-1}, as well as H–O–H bending near 1620–1630 cm^{-1} due to optimal interfacial bonding, homogeneously dispersed Si QDs in the Cs_2NaBiI_6 host matrix, and these two phenomena are maximized at this ratio. In contrast, Fig. 5d images a situation of significant band broadening and saturation as well as slight peak shifts in the high frequency region for Si QDs at loadings >3 wt%, suggesting over-aggregation of the Si QDs and complete failure to sustain the globally uniform bonding network. FTIR exposes the critical benefit that the 3 wt% Si QDs-doped composite (Fig. 5c) gives us with the perovskite in regards of chemical interconnectivity, where those Si QDs are well tethered directly to a stable covalent-like oxygen bridge to the surface of this pervoskite as represented. More evidently, the superior bonding between the polymer and perovskite at 3 wt% is vital for semiconductor device applications, particularly in perovskite solar cells as it enables efficient charge carrier transfer (without them being trapped), overcomes interfacial trap states, passivates surface defects and achieves long-term environmental stability while the lower connectivity at 1 wt% (Fig. 5b) does not provide sufficient passivation of surface states and the aggregated morphology stemming from a higher weight proportion of fillers in 5wt% introduces recombination centers and mechanical instability.

The optical absorption characteristics of pristine Cs_2NaBiI_6 perovskite and its Si QDs-doped composites (1, 3, and 5 wt%) were obtained from UV-Vis absorption spectroscopy as shown in Fig. 6. The absorbing spectra for the pristine Cs_2NaBiI_6 displayed in Fig. 6a show a sharp absorption edge (indicating the intrinsic band to band transition of the double perovskite) in the visible region and relatively low absorbance intensity beyond the edge indicating minimal contributions from secondary phases. When doped with 1 wt% Si QDs (Fig. 6b), a weak increase in absorbance in the whole visible spectrum occurs, and a minor red shift of edges of absorption that suggests the first practical incorporation of Si QDs performing as additional light-harvesting centers. Fig. 6c (3 wt% Si QDs) also exhibits the most considerable overall absorbance intensity(400–1000 nm), and the absorption edge is markedly broadened and red-shifted relative to that of pure Cs_2NaBiI_6 (up to approximately 820 nm for FWHM 90%) with their higher intensitiesafter QD doped into matrix, owingto better light scattering, effective charge-carrier generation, and intimate electronic coupling between Si QDs and the Cs_2NaBiI_6matrix. By comparison, the spectrum from Si QDs-5wt% (Fig. 6d) shows a reduced absorbance intensity compared to its analogue at 3 wt%, together with broadened spectral features and

an additional shoulder-like feature in the longer wavelength region that can be explained by over aggregation of Si QD- this not only leads to greater light scattering losses, but also enhances non-radiative recombination through defect-related sub-bandgap states [38,39]. The main benefit you can get from the absorption analysis is that the optimally prepared composite doped with 3 wt% Si QDs achieves a good compromise between enhanced light harvesting and few losses caused by aggregation. From the practical viewpoint for perovskite solar cells, the enhanced absorbance and broader spectral response of 3 wt% sample are directly converted into higher photocurrent generation on the one hand while inferior absorption at 5 wt% would lead to compromised device performance resulting from more recombination and poor charge extraction on another.

CONCLUSION

The lead-free double perovskite Cs_2NaBiI_6 was successfully synthesized using a solution-based method, and silicon quantum dots (Si QDs) were incorporated at 1, 3, and 5 wt%. The morphological analysis on SEM and TEM investigations indicates that the 3 wt% Si QDs-doped sample shows the best surface morphology, uniform distribution of QDs and excellent interfacial contact, whereas significant agglomeration and surface damage are observed in the 5 wt% sample. FTIR spectroscopy showed successful chemical grafting of Si QDs onto the perovskite matrix (via Si–O–Si linkages) and the 3 wt% sample exhibited the strongest interfacial bonding. From UV-Vis absorption spectroscopy, the 3 wt% composite exhibited higher absorbance intensity as well as a remarkable red shift which confirms better light harvesting. Combined, the 3 wt% Si QDs-doped Cs_2NaBiI_6 is revealed to deliver an ideal balance of morphology homogeneity, chemical connectivity and optical performance, thus making it a top-tier candidate for perovskite solar cells and any other optoelectronic devices.

CONFLICT OF INTEREST

The authors declare that there is no conflict of interests regarding the publication of this manuscript.

REFERENCES

1. Liu M, Wan Q, Wang H, Carulli F, Sun X, Zheng W, et al. Suppression of temperature quenching in perovskite nanocrystals for efficient and thermally stable light-emitting diodes. Nature Photonics. 2021;15(5):379-385.
2. Liu Y, Rong X, Li M, Molokeev MS, Zhao J, Xia Z. Incorporating Rare-Earth Terbium(III) Ions into $Cs_2AgInCl_6$:Bi Nanocrystals toward Tunable Photoluminescence. Angew Chem Int Ed. 2020;59(28):11634-11640.
3. Liu Y, Nag A, Manna L, Xia Z. Lead-Free Double Perovskite $Cs_2AgInCl_6$. Angew Chem. 2021;133(21):11696-11707.
4. Faleh FK, Bardan KH, Abdul-Hussein WA. DFT-driven insights into the structural, mechanical, electronic, optical, and thermoelectric properties of Ba_2XRhO_6 (X=Ta, V) double perovskites. Solid State Commun. 2026;415:116475.
5. Lead-Free $Cs_4CuSb_2Cl_{12}$ Layered Double Perovskite Nanocrystals. American Chemical Society (ACS).
6. Jin S, Li R, Huang H, Jiang N, Lin J, Wang S, et al. Compact ultrabroadband light-emitting diodes based on lanthanide-doped lead-free double perovskites. Light: Science and Applications. 2022;11(1).
7. Hossain MK, Samajdar DP, Das RC, Arnab AA, Rahman MF, Rubel MHK, et al. Design and Simulation of Cs_2BiAgI_6 Double Perovskite Solar Cells with Different Electron Transport Layers for Efficiency Enhancement. Energy and Fuels. 2023;37(5):3957-3979.
8. Daem N, Dewalque J, Kim DK, Spronck G, Attwood M, Wade J, et al. Improved Photovoltaic Performances of Lead-Free $Cs_2AgBiBr_6$ Double Perovskite Solar Cells Incorporating Tetracene as Co-Hole Transport Layer. Solar RRL. 2023;7(17).
9. Ali HH, Al-Bahrani MR. Enhancing Optical and Structural Properties of Lead-Free Cesium Europium Halide Perovskite Nanocrystals via Carbon Quantum Dots. Ann Chim - Sci Mat. 2025;49(3):291-297.
10. Creutz SE, Crites EN, De Siena MC, Gamelin DR. Colloidal Nanocrystals of Lead-Free Double-Perovskite (Elpasolite) Semiconductors: Synthesis and Anion Exchange To Access New Materials. Nano Lett. 2018;18(2):1118-1123.
11. Ali HH, Aziz SMA, Taha AB, Nayef UM. Impact of carbon quantum dots incorporation in electron transport layer on the performance of $CsPbBr_3$ -based perovskite solar cells. Int J Mod Phys B. 2026;40(11).
12. Bekenstein Y, Dahl JC, Huang J, Osowiecki WT, Swabeck JK, Chan EM, et al. The Making and Breaking of Lead-Free Double Perovskite Nanocrystals of Cesium Silver–Bismuth Halide Compositions. Nano Lett. 2018;18(6):3502-3508.
13. Aziz SMA, Ali HH, Taha AB, Muayad MW, Salih CN, Nayef UM. Structural, optical, and electronic characterization of Fe_3O_4@ZnO core–shell nanostructures synthesized by laser ablation. Journal of Materials Science: Materials in Electronics. 2026;37(15).
14. Abdul-Hussein WA, Hanoon FH, Al-Badry LF. Control the electronic and optical properties of AlN nanosheet by the electric field. Results in Optics. 2023;11:100423.
15. Ali AS, Roomi AB, Ali HH, Fadaam SA. Comparative study between summer and winter of selected Heavy elements in water, sediment and two species of aquatic plants collection from Al-Gharraf River near Al- Gharraf oil field- Thi-Qar province – Iraq. IOP Conference Series: Materials Science and Engineering. 2020;928(6):062010.
16. Ning Z, Gong X, Comin R, Walters G, Fan F, Voznyy O, et al. Quantum-dot-in-perovskite solids. Nature. 2015;523(7560):324-328.
17. Amino Acid Double-Passivation-Enhanced Quantum Dot Coupling for High-Efficiency FAPbI3 Perovskite Quantum Dot Solar Cells. American Chemical Society (ACS).
18. abd JS, Hasan KH, Mhawes AJ, Ali HH, Abdulzahraa EM. The Use of Erubium Yag (Er: YAG) Laser to Treat Burns and Study Laser Effect on the Enviroment. Indian Journal of Public Health Research and Development. 2019;10(10):2663.
19. Sawires EF, Ismail Z, Samir M, Agour AM, Amer FZ, Nageh H, et al. Exploring various Integration Methods of carbon quantum dots in $CsPbCl_3$ perovskite solar cells for enhanced power conversion efficiency. Journal of Materials Science: Materials in Electronics. 2024;35(11).
20. Abdul-Hussein WA, Hanoon FH, Al-Badry LF. Designing sub-5 nm monolayer AlP MOSFETs. Micro and Nanostructures. 2023;176:207524.